Modeling the global bomb tritium transient signal with the AGCM LMDZ-iso: A method to evaluate aspects of the hydrological cycle

Alexandre Cauquoin, P. Jean-Baptiste, C. Risi, É. Fourré, A. Landais

AGU PUBLICATIONS

JGR

Journal of Geophysical Research: Atmospheres

RESEARCH ARTICLE
10.1002/2016JD025484

Key Points:
- The anthropogenic tritium injected by each of the atmospheric nuclear tests has been estimated and implemented in the AGCM LMDZ-iso
- LMDZ-iso correctly reproduces the general shape of the temporal evolution of tritium in precipitation between 1950 and 2008
- Tritium model-data comparisons provide an additional tool to test the stratospheric residence time in the models

Supporting Information:
- Supporting Information S1
- Table S1

Correspondence to:
A. Cauquoin,
alexandre.cauquoin@awi.de

Citation:
Cauquoin, A., P. Jean-Baptiste, C. Risi, É. Fourré, and A. Landais (2016), Modeling the global bomb tritium transient signal with the AGCM LMDZ-iso: A method to evaluate aspects of the hydrological cycle, *J. Geophys. Res. Atmos.*, *121*, 12,612–12,629, doi:10.1002/2016JD025484.

Received 21 JUN 2016
Accepted 8 OCT 2016
Accepted article online 14 OCT 2016
Published online 5 NOV 2016

Modeling the global bomb tritium transient signal with the AGCM LMDZ-iso: A method to evaluate aspects of the hydrological cycle

A. Cauquoin[1,2], P. Jean-Baptiste[2], C. Risi[1], É. Fourré[2], and A. Landais[2]

[1]Laboratoire de Météorologie Dynamique/Institut Pierre-Simon Laplace (LMD/IPSL), CNRS, Sorbonne Universités, UPMC Univ Paris 06, Paris, France, [2]Laboratoire des Sciences du Climat et de l'Environnement, UMR 8212, CEA-CNRS-UPS/IPSL, Gif-sur-Yvette, France

Abstract Improving the representation of the hydrological cycle in atmospheric general circulation models (AGCMs) is one of the main challenges in modeling the Earth's climate system. One way to evaluate model performance is to simulate the transport of water isotopes. Among those available, tritium is an extremely valuable tracer, because its content in the different reservoirs involved in the water cycle (stratosphere, troposphere, and ocean) varies by order of magnitude. Previous work incorporated natural tritium into Laboratoire de Météorologie Dynamique Zoom (LMDZ)-iso, a version of the LMDZ general circulation model enhanced by water isotope diagnostics. Here for the first time, the anthropogenic tritium injected by each of the atmospheric nuclear bomb tests between 1945 and 1980 has been first estimated and further implemented in the model; it creates an opportunity to evaluate certain aspects of LDMZ over several decades by following the bomb tritium transient signal through the hydrological cycle. Simulations of tritium in water vapor and precipitation for the period 1950–2008, with both natural and anthropogenic components, are presented in this study. LMDZ-iso satisfactorily reproduces the general shape of the temporal evolution of tritium. However, LMDZ-iso simulates too high a bomb tritium peak followed by too strong a decrease of tritium in precipitation. The too diffusive vertical advection in AGCMs crucially affects the residence time of tritium in the stratosphere. This insight into model performance demonstrates that the implementation of tritium in an AGCM provides a new and valuable test of the modeled atmospheric transport, complementing water stable isotope modeling.

1. Introduction

The water cycle is a key component of the Earth's climate system. Modeling the time responses of this cycle and the implied physical processes (evaporation, precipitation, and atmospheric transport) challenges the atmospheric general circulation models (AGCMs) used to study the climate system and to project future climate. One method of evaluating the performance of these models is to simulate the transport of the water stable isotopes ($H_2^{16}O$, HDO, $H_2^{18}O$, and $H_2^{17}O$) [*Joussaume et al.*, 1984; *Jouzel et al.*, 1987; *Hoffmann et al.*, 1998; *Mathieu et al.*, 2002; *Noone and Simmonds*, 2002; *Lee et al.*, 2007; *Schmidt et al.*, 2007; *Yoshimura et al.*, 2008; *Tindall et al.*, 2009; *Risi et al.*, 2010, 2013; *Werner et al.*, 2011], which are tracers of the past and present-day hydrological cycle.

Tritiated water (HTO) is another useful tracer. Tritium (T) is naturally produced by the interaction of cosmic radiation with nitrogen atoms in the upper atmosphere, at an average rate of 3200 atoms m^{-2} s^{-1} [*Masarik and Beer*, 2009], and has a radioactive half-life of 12.32 ± 0.02 years [*Lucas and Unterweger*, 2000]. The vast majority of this natural (i.e., cosmogenic) tritium, which amounts to a steady state global inventory of 3.6 kg [*Fourré et al.*, 2006], enters the hydrological cycle in the form of tritiated water molecules (HTO) [*Gat et al.*, 2001]. Because of this upper atmospheric production and different tritiated water concentrations in the main reservoirs involved in the water cycle (stratosphere, troposphere, and ocean considered in this study), HTO is an extremely valuable marker for the fluxes between these reservoirs. For example, the natural tritium content of stratospheric water vapor has been estimated to be some $5–9 \times 10^5$ TU (tritium units, where 1 TU corresponds to T/H ratio of 10^{-18}) [*Ehhalt et al.*, 2002; *Fourré et al.*, 2006], which is several orders of magnitude greater than the natural tritium level in precipitation (a few TU only [*IAEA*, 2016]). This large stratospheric reservoir also makes tritium an extremely valuable tracer for mapping the intrusion of stratospheric air masses into

the troposphere, in particular, over Antarctica, a region under the influence of the polar vortex [*Taylor*, 1968; *Jouzel et al.*, 1979, 1982; *Wagenbach et al.*, 1998; *Fourré et al.*, 2006].

Furthermore, vast amounts of anthropogenic tritium from nuclear tests were injected into the atmosphere, mainly during the 1950–1960s (520–550 kg [*Michel*, 1976; *United Nations Scientific Committee on the Effects of Atomic Radiation (UNSCEAR)*, 2000], ~90% of which went into the stratosphere). These tests have caused a huge "tritium peak" (or "bomb peak") to be measured in precipitation [*IAEA*, 2016]. For example, the precipitation in Vienna reached concentrations of tritium 700–800 times higher in 1963–1964 than those at the end of the 2000s. Since the Nuclear Test Ban Treaty in 1963 the level of tritium measured in precipitation has been steadily decreasing due to radioactive decay and dilution in the world oceans. The concentration of tritium in precipitation has been continuously monitored by the Global Network of Isotopes in Precipitation (GNIP, database available through the International Atomic Energy Agency) for the last 60 years. The data suggest that tritium levels in precipitation are now close to their prenuclear test values, which can be estimated from ice cores and a few pre-bomb samples of precipitation [*Cauquoin et al.*, 2015].

The occurrence of natural tritium has already been implemented in the Laboratoire de Météorologie Dynamique Zoom (LMDZ) Atmospheric General Circulation Model [*Cauquoin et al.*, 2015] developed at LMD [*Hourdin et al.*, 2006, 2013]. This isotopic version is hereafter called LMDZ-iso [*Risi et al.*, 2010]. This first step was necessary to test the simulated distribution of tritium in the atmosphere due to climatic processes. The transport of tritium and its spatial/seasonal variability was analyzed under steady state cosmogenic tritium inputs, i.e., without the massive increase of tritium due to nuclear weapon testing.

Here we further test the realism of the water cycle dynamics modeled by LMDZ-iso through a tritium model-data comparison that includes the anthropogenic component of this tracer coming from the nuclear weapon tests. With the exception of the pioneering study by *Koster et al.* [1989] with a very simplified bomb tritium input function and extremely limited resolution and simulation time, this is the first time that a detailed bomb tritium input is presented and implemented in an AGCM. In fact, the atmospheric input of the huge and well-dated transient thermonuclear tritium in LMDZ-iso is expected to help in testing the time response of the modeled hydrological cycle and better decipher the influences of horizontal tropospheric transport versus vertical advection between the stratosphere and the troposphere. Modeling such an anthropogenic signal relies, however, on a precise inventory of the tritium inputs during the bomb tests. While details of the atmospheric bomb tests (including dates, location, and fission and fusion yields) are now available [*UNSCEAR*, 2000], the corresponding records of the amount of atmospheric tritium released by each individual test are not. The present study fills this gap and provides for the first time an estimate of the time evolution of the atmospheric bomb tritium emissions throughout the period of atmospheric tests.

The outline of this paper is as follows. Section 2 briefly outlines the description of the isotopic processes included in LMDZ-iso. We also give details of the methodology used to derive the amount of tritium released into the atmosphere by each individual nuclear detonation, based on its fission and fusion yields, as well as the elevation and thickness of the corresponding nuclear cloud. We also describe the additional oceanic boundary conditions that have been implemented in the model. We then describe the various simulations performed and the tritium data used for validation. In section 3, we evaluate the simulated temporal variations of tritium in precipitation and in water vapor between 1950 and 2008 at different representative and well-documented areas such as Europe and Antarctica. In section 4, we use the comparison between the observed and modeled variability of tritium to identify and better constrain the driving mechanisms of the tritium peak in precipitation and of its decay within the hydrological cycle. With this aim, we apply specific sensitivity tests and evaluate the resulting effects on several well-documented regions.

2. Model Simulations and Data Sets

2.1. LMDZ-iso and Isotopic Processes

Following *Cauquoin et al.* [2015] in modeling natural tritium, we use here the LMDZ model version LMDZ5a [*Dufresne et al.*, 2013]. The dynamical part is based on a discrete latitude-longitude grid, at the standard resolution of 2.5° × 3.75°. The advection of water in its vapor and condensed states is calculated using the *van Leer* [1977] scheme. An error has been found and corrected in this advection scheme of our version of LMDZ-iso, with the result that the properties of the air in the target grid box are the same as in the source grid box, instead of being the result of a linear combination between the two boxes involved. The erroneous scheme, so-called "upstream scheme," is too diffusive [*Hourdin and Armengaud*, 1999] and affects all water isotopes,

including the values of our simulated natural tritium content in water [*Cauquoin et al.*, 2015], with as the main consequence a humid bias at the poles and especially in the polar stratosphere. The correction of this error in the advection scheme did not change the main results and the conclusions from our previous study and even improved the agreement with the present observations because the −30% correction coefficient applied to the cosmogenic production of tritium [*Masarik and Beer*, 2009] in our previous study is no longer necessary. A dedicated note will be issued to address the consequences of this correction in the advection scheme for other modeled parameters.

To ensure a realistic description of the stratosphere and of the Brewer-Dobson circulation, the model is run in its "stratospheric" version, i.e., with 39 layers in the vertical, including 22 located above the 200 hPa pressure level [*Lott et al.*, 2005]. The physical package, described in detail by *Hourdin et al.* [2006] and *Dufresne et al.* [2013], includes the Emanuel convective parameterization [*Emanuel*, 1991] coupled to the *Bony and Emanuel* [2001] cloud scheme.

Following *Risi et al.* [2010], LMDZ-iso uses the same physical and dynamical descriptions of the HTO molecule as for the other water isotopes. Due to mass and symmetry differences, the various isotopic forms of the water molecule ($H_2^{16}O$, $H_2^{18}O$, HDO, $H_2^{17}O$, and HTO) have slightly different physical properties (e.g., saturation vapor pressure and molecular diffusivity) and are therefore redistributed between the vapor and condensed phases at each phase change differently, depending on atmospheric conditions (temperature, vapor saturation, etc.). The implementation of the water stable isotopes in LMDZ-iso and of their associated isotopic effects (kinetic and equilibrium) has been extensively described by *Risi et al.* [2010] and *Bony et al.* [2008]. Concerning the HTO molecule, the equilibrium fractionation coefficients between vapor and liquid water or ice are given by *Koster et al.* [1989]. We take into account the kinetic effects during the evaporation of water from the sea surface following *Merlivat and Jouzel* [1979] and during snow formation following [*Jouzel and Merlivat*, 1984], with the supersaturation parameter S set to 0.004 [*Risi et al.*, 2010]. More details about the parameterization of the isotopic processes influencing HTO distribution are given by *Cauquoin et al.* [2015].

2.2. Implementation of the Bomb Tritium Input Function

2.2.1. Global Production of Bomb Tritium

The inventory of tritium arising from atmospheric nuclear tests can be determined either from the estimation of the tritium production per megaton (Mt) of fission and fusion yields of the nuclear devices multiplied by the total yield of nuclear tests or from the summation of the tritium present in the various compartments of the hydrosphere based on environmental measurements. Table 1 summarizes the various estimates published in the literature. The latest figures converge toward the value presented by UNSCEAR in its 2000 report which reviewed the global inventory of radionuclides produced and globally dispersed by atmospheric nuclear testing and the assessment of the radiation dose induced to the public: 186,000 PBq corresponding to 520 kg of T. This figure, based on nuclear weapon yields, is remarkably close to *Michel*'s estimate [1976] of 550 ± 160 kg, based on the global inventory of tritium in the environment. Note that HT gas can also leak from underground nuclear tests and military tritium facilities [*Happell et al.*, 2004]. Based on HT atmospheric data, *Happell et al.* [2004] calculated a global total of atmospheric tritium that peaked at 1.3 kg in 1975 and has dropped since then to less than 0.2 kg (2002 value). This tritiated hydrogen in the atmosphere is mainly (80%) taken up by soils and transformed to HTO by bacterial oxidation [*Hauglustaine and Ehhalt*, 2002; *Constant et al.*, 2009]. Therefore, it can be neglected in the HTO atmospheric budget. Before 1980, atmospheric releases of HTO by the nuclear power industry are negligible. After 1980, 0.7 kg of tritium on average [*UNSCEAR*, 2000] have been released each year into the atmosphere (in comparison, natural production is ∼0.2 kg per year [*Craig and Lal*, 1961]). However, as shown by tritium measurements around nuclear plants [*Jean-Baptiste et al.*, 2007] most of this tritium is scavenged locally by precipitation. So these tritiated effluents are not likely to significantly influence tritium concentration in precipitation away from their release point.

2.2.2. Tritium Production as a Function of Fission and Fusion Yields of Nuclear Tests

Following the end of the Cold War, details on nuclear tests (location, date, altitude of detonation, fission and fusion yields, etc.) were made available to the public [*U.S. Department of Energy Nevada Operations Office*, 2000; *Kirchmann*, 2000; *UNSCEAR*, 2000]. It is therefore possible to construct a detailed timetable of tritium injection into the atmosphere including each individual test, provided that the amount of tritium produced by each nuclear detonation is known. The UNSCEAR nuclear bomb test data set breaks down the total energy released by each individual test into its fission and fusion component [*UNSCEAR*, 2000, Annex C, Table 1]. However, tritium production per megaton of fission and fusion yields reported in the literature varies over a fairly wide range. Therefore, an average tritium production per megat of fission and fusion yields has to be determined.

Table 1. Global Tritium Inventories Published in the Literature[a]

Reference	Tritium Input (kg of T)	Method	Date of Inventory	Remark
Martell [1963]	124	1	1961	–
Eriksson [1965]	196	1	1962	–
Miskel [1973]	828	1	1962	–
Schell et al. [1974]	816	1	1962	–
NRCP [1979]	362	1	1962	–
UNSCEAR [2000]	520	1	1962	–
Michel [1976]	550 ± 160	2	1970	Total hydrosphere
Weiss and Roether [1980]	407	2	1972	Oceans only
Broecker et al. [1986]	460	2	1973-1978	Oceans only

[a]Methods 1 and 2 refer to weapon yields and environmental data decay-corrected to 1960, respectively.

Tritium released by atmospheric nuclear detonations originates from the following main sources: (1) uranium ternary fission; $^{14}N(n,^3H)^{12}C$ reactions induced by (2) fission and (3) fusion neutrons of atmospheric nitrogen; and (4) residual tritium produced by neutrons captured by lithium in the explosive.

Therefore, the global tritium production NT (in mol) can be written as follows:

$$N_T = (a_1 + a_2)P_{\text{fission}} + (a_3 + a_4)P_{\text{fusion}} \tag{1}$$

where P_{fission} and P_{fusion} are the global fission and fusion yields of nuclear weapons (P_{fission} = 189.403 Mt and P_{fusion} = 250.56 Mt [*UNSCEAR*, 2000]) and a_i coefficients are the tritium production (in mol T Mt^{-1}) according to the four mechanisms listed above. N_T amount corresponds to 520 kg or 173,333 moles of tritium (see above).

Coefficient a_1 (uranium ternary production) is small (a_1 = 0.019 mol T Mt^{-1}) based on 1.4×10^{26} fissions Mt^{-1} [*Miskel*, 1973] and 0.8×10^{-4} atoms of tritium per fission [*Sloth et al.*, 1962] and could even be neglected.

Since bomb carbon-14 (^{14}C) is also produced by $^{14}N(n,p)^{14}C$ reactions on atmospheric nitrogen (see mechanisms 2 and 3 above), coefficients a_2 and a_3 can be determined by scaling them to those for ^{14}C, taking into account the respective neutron cross sections of the $^{14}N(n,p)^{14}C$ and $^{14}N(n,^3H)^{12}C$ reactions. The cumulative bomb ^{14}C production $N_{^{14}C}(t)$ at time t can be written as

$$N_{^{14}C}(t) = b_2 \sum_t y_{\text{fission}} + b_3 \sum_t y_{\text{fusion}} \tag{2}$$

where $\sum_t y_{\text{fission}}$ and $\sum_t y_{\text{fusion}}$ are the cumulative fission and fusion yields between t_0 and t.

The various estimates of the total bomb ^{14}C inventory, based on environmental data or on carbon cycle models, agree on the value $N_{^{14}C} = 10^5$ mol (±10%) [*Hesshaimer et al.*, 1994; *Lassey et al.*, 1996; *Jain et al.*, 1997; *Naegler and Levin*, 2006]. Using the *UNSCEAR* [2000] nuclear bomb test data set and equation (2), the coefficients b_2 and b_3 that produce the best fit to time evolution of the radiocarbon inventory from 1945 to 1965 have been determined, giving b_2 = 117 and b_3 = 320 mol ^{14}C Mt^{-1} (Figure 2, right).

Figure 1 displays the cross sections for the two reactions, $^{14}N(n,p)^{14}C$ and $^{14}N(n,^3H)^{12}C$, as a function of neutron energy, as well as the energy distribution of fission neutron, $P(E)$, and the energy (14 MeV) of fusion neutrons created by D-T reactions. It follows that the production ratio of ^{14}C to tritium by fission neutrons is

$$b_2/a_2 = \frac{\int \sigma_{^{14}C} P(E)\mathrm{d}E}{\int \sigma_T P(E)\mathrm{d}E} = 44.5 \tag{3}$$

giving a_2 = 2.63 mol T Mt^{-1}. For the 14 Mev fusion neutrons, the production ratio is simply $b_3/a_3 = \sigma_{^{14}C}/\sigma_T$ (at 14 Mev) = 1.54, giving a_3 = 207.8 mol T Mt^{-1}. Finally, coefficient a_4 can be determined using equation (1):

$$a_4 = \frac{N_T - (a_1 + a_2)P_{\text{fission}} - a_3 P_{\text{fusion}}}{P_{\text{fusion}}} \tag{4}$$

giving a_4 = 482 mol T Mt^{-1}.

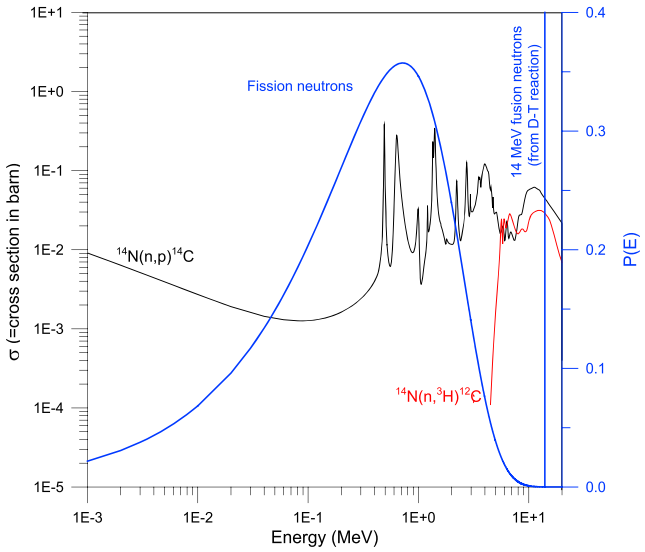

Figure 1. Cross section (expressed in barn, equivalent to 10^{-28} m^2) of $^{14}N(n,p)^{14}C$ (in black) and $^{14}N(n,^3H)^{12}C$ (in red) reactions as a function of neutron energy (ENDF data base from *Chadwick et al.* [2011]) and energy distribution of fission neutrons (in blue). The number of fission neutrons with an energy between E and $E + dE$ is proportional to $P(E)dE$.

Coefficients a_i are summarized in Table 2, with their value in mol T Mt^{-1} and g T Mt^{-1}. The corresponding cumulative bomb tritium production is shown in Figure 2. One can deduce that atmospheric tritium releases are dominated by fusion, with a tritium production of 2.07 kg Mt^{-1}, against 8×10^{-3} kg Mt^{-1} for fission, in full agreement with the *UNSCEAR* [2000] estimates. As a whole, over the 520 kg of tritium produced by the atmospheric nuclear tests, 518.5 kg (99.7%) were due to fusion and only 1.5 kg (0.3%) to fission.

2.2.3. Height of the Tritium Injection

The altitude at which tritium is released is a key parameter for modeling tritium in an AGCM. In particular, a realistic partitioning between the amounts released into the troposphere and into the stratosphere is very important, since tritium has a residence time of several years in the stratosphere before being transferred across the tropopause and being incorporated into precipitation. For a given explosion height, the height of the nuclear cloud depends on buoyancy forces and thus on the amount of energy released by the explosion and on the atmospheric vertical density field. Figure 3 displays available literature data for the maximum height and vertical extent of a nuclear cloud as a function of the energy of the detonation, as well as the curve derived from *Machta*'s semiempirical theory for tropical latitudes [*Machta*, 1950; *Kellogg et al.*, 1957]. Figure 3 shows that *Machta*'s curve clearly underestimates the height of the cloud. Moreover, probably because of the substantial scatter in the data, it does not show any clear evidence of a significant difference of height between tropical and midlatitude explosions. Therefore, for the altitude and extent of the atomic cloud in the model, we empirically adopt polynomial fits (solid lines in Figure 3). With this formulation, 92% of the tritium production is injected into the stratosphere, in good agreement with the *UNSCEAR* [2000] estimate of 89.9%.

2.2.4. Implementation in LMDZ-Iso

The two steps presented above allow us to deduce the amount of tritium injected into the high atmosphere and the height of the nuclear cloud for each individual atmospheric nuclear test between 1945 and 1980 whose date, localization, and yield are known (see supporting information). We removed two nuclear bomb tests from this list because their heights of injection were too high (80 and 100 km high, highlighted in red in Table S1) compared to the maximum altitude in the model (around 52 km high). These two nuclear tests

Table 2. Summary of Our Estimate of Tritium Yields of Atmospheric Nuclear Tests

Production Mechanism	Tritium Yield (mol T Mt^{-1})	Tritium Yield (g T Mt^{-1})
(1) Ternary fissions	0.019	0.06
(2) $^{14}N(n,^3H)^{12}C$ for fission neutrons	2.62	7.9
(3) $^{14}N(n,^3H)^{12}C$ for fusion neutrons	207.8	623.4
(4) Residual tritium in the explosive	482	1446

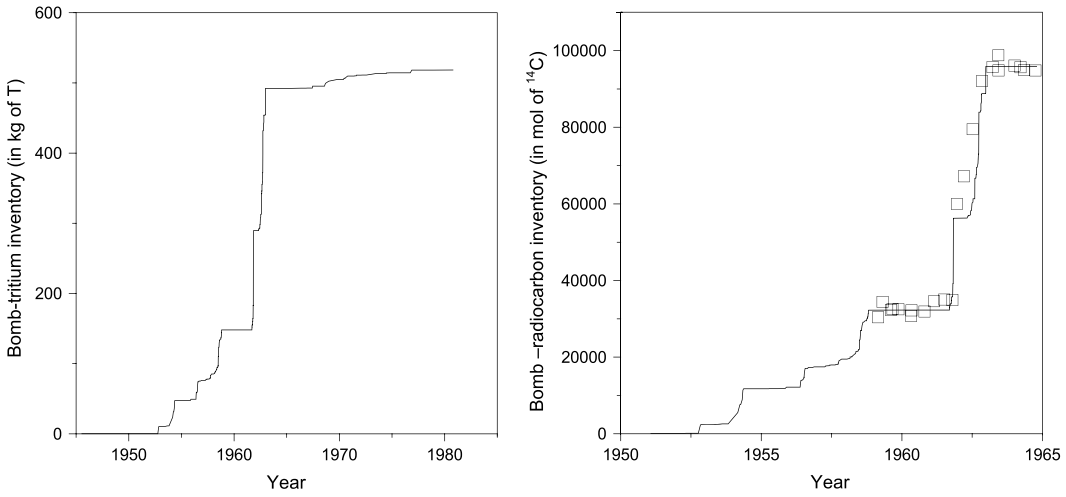

Figure 2. (left) Cumulative bomb tritium production from the UNSCEAR nuclear bomb test data set using tritium yields of Table 2. (right) Bomb ^{14}C inventories during the moratorium on nuclear tests (1959–1961) and at the end of USA-USSR atmospheric tests (open squares) and cumulative ^{14}C production (black line) according to equation (2) for $b_2 = 117$ and $b_3 = 320$ mol ^{14}C Mt^{-1} (inventories are based on ^{14}C measurements in the troposphere and stratosphere plus model results for biosphere and ocean [*Naegler*, 2005]).

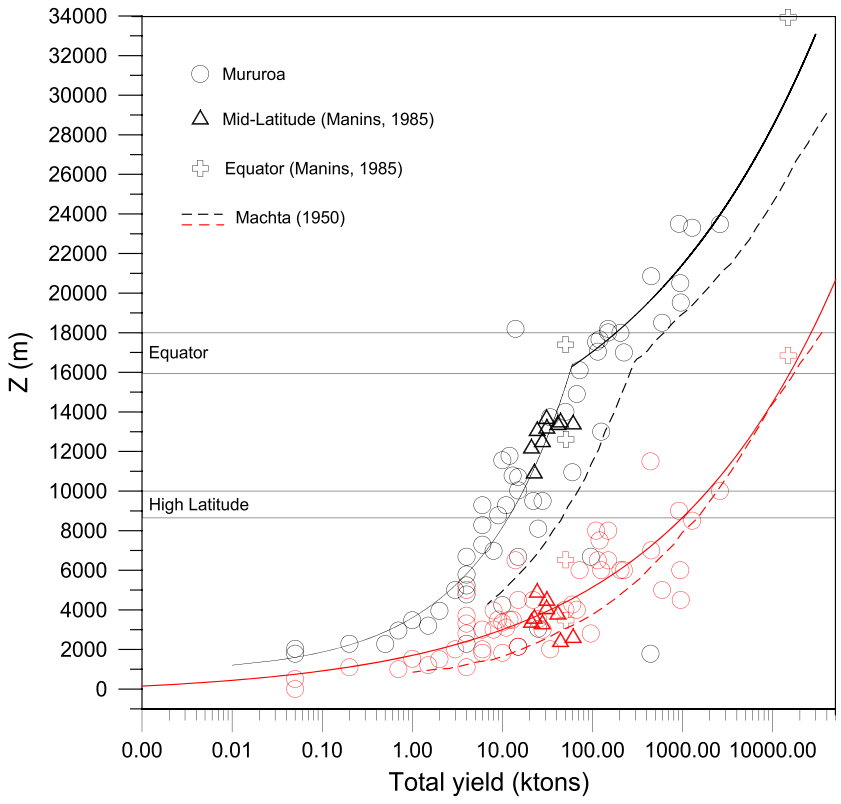

Figure 3. Maximum height (in black) and vertical extent (in red) of a nuclear cloud as a function of the energy of the detonation. The dotted curves are derived from Machta's theory for a tropical atmosphere [*Machta*, 1950; *Kellogg et al.*, 1957]. Solid curves are the polynomial fits considered from this study. The horizontal black lines refer to the altitude ranges of the tropopause at the equator and high latitudes.

injected 4.46 kg of tritium into the atmosphere, which represents 0.86% of our anthropogenic tritium input signal. Omitting these two nuclear tests gives a total of 513.9 kg of tritium injected into the atmosphere during our simulations. This anthropogenic production of tritium has then been used as an input in LMDZ-iso in the following way. For each nuclear test, the corresponding amount of bomb tritium injected into the atmosphere is evenly spread during the entire day. According to the localization of the nuclear test, we select the corresponding closest horizontal mesh (i.e., latitudinal and longitudinal coordinates). Then, the bomb tritium input is uniformly distributed in an air column between the first layers below and above the nuclear cloud. This assumption is tested later in the manuscript with a sensitivity test on the height of injection of bomb tritium in the atmosphere and its consequences on the tritium concentration in precipitation and in stratospheric water vapor.

2.3. Boundary Conditions on Tritium at the Surface of the Oceans

Modeling tritium in an AGCM requires proper oceanic boundary conditions. Due to radioactive decay and dilution by the oceans, tritium concentration at the ocean surface has decreased rapidly since the bomb test period. We reconstructed the time evolution of the oceanic boundary conditions for tritium using all available tritium measurements at the ocean surface during the whole period of interest. These include multiple data sets, which represent more than 2500 collected data points. To provide monthly maps of surface oceanic tritium between 1950 and 2004, we have used the methodology of *Broecker et al.* [1986], i.e., the data were split into specific latitudinal bands where surface tritium concentrations can be considered "homogeneous." For each latitudinal band, the data were then fitted and interpolated using polynomial functions (Figure S2). In this way, we produced the necessary maps of tritium at the ocean surface for each month of simulation. Finally, we smoothed the maps by applying a Gaussian low-pass filter. For the years before 1950 and after 2004, we considered that the distributions of tritium content at surface of the ocean were the same as of January 1950 and December 2004, respectively. Additional information about the methodology and the sources can be found in the supporting information [*Andrié et al.*, 1988; *Bainbridge*, 1963; *Bonisch and Schlosser*, 1995; *Bowen and Roether*, 1973; *Broecker et al.*, 1986; *CCHDO*, 2016; *Dockins et al.*, 1967; *Dorsey and Peterson*, 1976; *Dreisigacker and Roether*, 1978; *Gargett et al.*, 1986; *Östlund et al.*, 1987; *Jenkins*, 1977, 1980, 1989, 1996; *Kakiuchi et al.*, 1999; *Landa et al.*, 1999; *Leboucher et al.*, 2007; *Michel and Williams*, 1973; *Michel and Suess*, 1975; *Michel et al.*, 1979; *Mulsow et al.*, 2003; *Östlund et al.*, 1969, 1986; *Östlund and Grall*, 1987; *Jean-Baptiste et al.*, 1998, 2004; *Povinec et al.*, 2004; *Roether et al.*, 1970; *Roether*, 1974; *Schlosser*, 1985; *Schlosser et al.*, 1995; *Tamuly*, 1974; *Top et al.*, 1998; *Zaucker*, 1988].

2.4. Simulations and Sensitivity Tests

As in *Cauquoin et al.* [2015], all our simulations were nudged by the horizontal winds from 20CR reanalyses [*Compo et al.*, 2011], which go back to 1871. The model starts running in 1940 from the equilibrium state with the cosmogenic production obtained from the previous study of *Cauquoin et al.* [2015]. The model then runs until 2008, and the outputs are evaluated with a focus on the period after the mid-1950s when the tritium content in precipitations began to be monitored more intensively following the beginning of the nuclear bomb tests.

We performed several simulations with different input parameters and boundary conditions to test the sensitivity of the model to the height of the bomb tritium injection, the tritium concentration at the surface of the oceans, and the properties of the advection scheme. More than the quantity of tritium released by a nuclear test, its height of injection in the atmosphere is a key parameter; this is because of the difference in residence time between the stratospheric and tropospheric compartments. In our simulation bomb tritium is linearly distributed over the height range of the nuclear cloud, but this assumption can be challenged. For example, in the carbon cycle model GRACE (Global Radiocarbon Exploration Model), *Naegler and Levin* [2006] prescribed an exponential distribution of the bomb radiocarbon with altitude within the nuclear cloud. To test the consequences of such uncertainties on the estimated tritium in precipitation in LMDZ-iso, we performed a simulation imposing bomb tritium injection only into the layer corresponding to the top of the nuclear cloud. This relatively extreme test allowed us to evaluate the effects of vertical atmospheric transport on the resulting modeled tritium concentration in water vapor and precipitation.

We also explored the influence of the oceanic boundary conditions. In this analysis, we ran a simulation with a uniform tritium content at the ocean surface of 0.2 TU (the value set for the simulation of natural tritium by *Cauquoin et al.* [2015], corresponding to an extrapolated estimate of pre-bomb tritium in the North Atlantic surface waters [*Dreisigacker and Roether*, 1978]). This distribution replaced the usual monthly tritium

concentration reconstruction. Finally, the tendency of the advection scheme to be more or less diffusive has been shown to strongly affect the tropospheric humidity and its isotopic composition [*Risi et al.*, 2012]. To test this effect, we performed sensitivity tests in which we replace the *van Leer* [1977] second-order advection scheme usually used in LMDZ-iso by the much simpler upstream scheme [*Godunov*, 1959]. The latter is much more diffusive, as explained in Appendix A and in section 2.1. To summarize, the main simulations were as follows: (1) "standard," with the bomb tritium production function as detailed above and our monthly reconstruction of tritium concentration at the ocean surface described in section 2.3; (2) "cloud_top," as (1) but all tritium from each nuclear test is injected into the upper layer of the nuclear cloud instead of being uniformly distributed over all the nuclear cloud; (3) "0.2TU," as (1) but with the ocean surface set at 0.2 TU throughout the simulation; (4) "advec_xy," same as (1) but with an upstream scheme on the horizontal plane (xy); and (5) "advec_z," same as (1) but with an upstream scheme on the vertical direction (*z*).

2.5. Description of the Available Tritium Data for Model-Data Comparison

In this study, we focus on the evaluation of the temporal evolution of modeled tritium content in precipitation and in water vapor during and after the era of atmospheric nuclear bomb testing. Therefore, well-resolved and continuous tritium data are needed throughout this period. In the GNIP water isotopes database of the *IAEA* [2016], only a few stations were monitored for tritium in precipitation throughout the whole period of interest. We have selected five stations representative of different precipitation regimes: Vienna (central Europe), Melbourne (South Pacific), Valentia Island (coastal Europe), Ottawa (northern America), and Halley Bay (Antarctica). For the tritium concentration in stratospheric water vapor, we used the data from *Ehhalt et al.* [2002]. It must be noted that these latter data are very limited in time and space, which makes the result of the comparison between our simulations and the observations more uncertain.

3. Results: Tritium in Precipitation and in Stratospheric Water Vapor

3.1. Tritium in Precipitation Between 1950 and 2008

To evaluate the LMDZ-iso simulation results, we analyze here the model capability to correctly simulate the temporal trend of tritium in precipitation between 1950 and 2008 (Figure 4) by comparing our simulation with the GNIP observations described in the previous section (also indicated in Figure S3). First, notice that LMDZ-iso reproduces the general shape of the tritium content in precipitation fairly well during our period of interest, with an increase of tritium content before the 1960s and a decrease after the bomb test ban treaty. This confirms that the implemented amounts of tritium released by the atmospheric nuclear tests are realistic.

Looking at differences between stations displayed in Figure 4, the Northern Hemisphere stations exhibit an initial increase by 2 to 3 orders of magnitude in their modeled tritium levels in precipitation during the years 1952–1953, followed by a lower increase until the beginning of 1959. The level then decreased, leading to a local minimum in 1961. This pattern, linked to the chronology of the bomb tests, is clearly visible in the tritium data from Ottawa and Valentia. Although tritium data are not available for Vienna before 1961, our simulated tritium is in agreement with the observations for the local minimum before the main bomb peak in 1962–1964. The shape of the 1962–1964 tritium bomb peak produced by LMDZ-iso is in relatively good agreement with the one observed in the data. Some differences, however, common to these three Northern Hemisphere stations, remain. First, LMDZ-iso overestimates the tritium content in precipitation during this period by factors of 2, 2.5, and 3.5 at Vienna, Valentia, and Ottawa, respectively. Furthermore, the curve of simulated tritium in precipitation exhibits two sharp peaks in February 1962 and 1963. These two peaks appear in the observations too, but the signal is much smoother and with a maximum, slightly shifted in time, in June 1963. After this maximum, the simulated tritium in precipitation follows an exponential decrease, sharply at first until the year 1990 and then more weakly (Valentia and Ottawa) as it asymptotically approaches the pre-bomb values. When we compare our Northern Hemisphere outputs with the observations, we notice that the simulated tritium in precipitation decreases too strongly after the bomb peak. As a consequence, LMDZ-iso underestimates the tritium in precipitation for the Northern Hemisphere, so that our simulated tritium in precipitation is closer to the pre-bomb values than it is in reality. This underestimation cannot be due to an error in our tritium input function because the peak is higher in our simulations than in the data. We did not take into account the tritiated emissions from nuclear power plants, but that is not a plausible explanation—these emissions are mostly scavenged locally by precipitation [*Jean-Baptiste et al.*, 2007] and so are not likely to significantly influence tritium concentration in precipitation away from their release point. To summarize, the simulated bomb tritium injected into the atmosphere (more than 90% into the stratosphere) is transferred too rapidly through the lower vertical layers to be sufficiently diluted in the atmosphere. This rapid

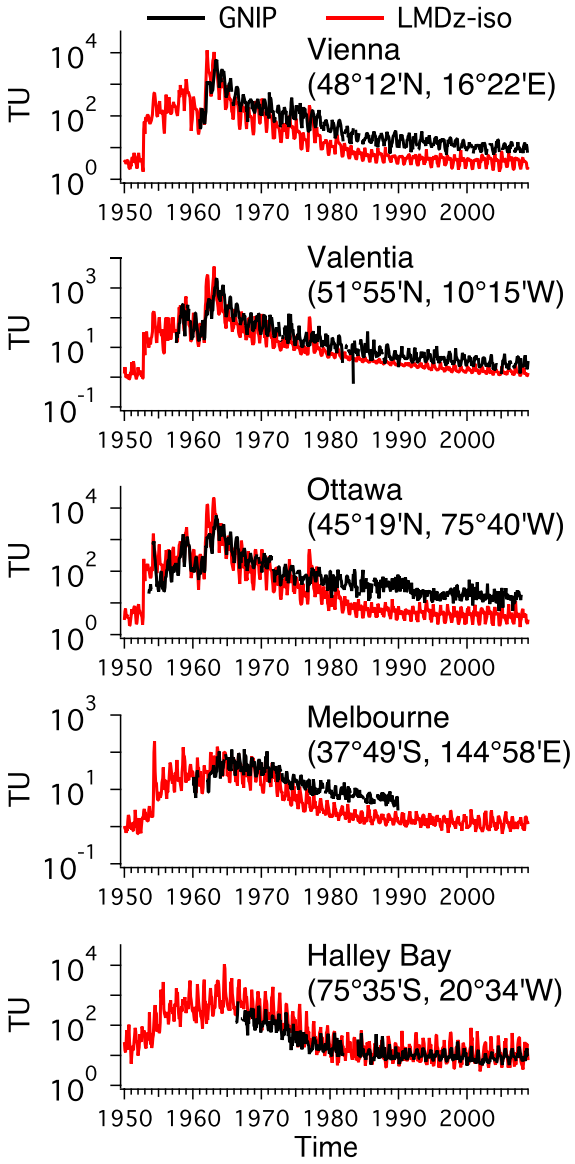

Figure 4. Monthly values of tritium in precipitation at Vienna, Valentia, Ottawa, Melbourne, and Halley Bay between 1950 and 2008. The black line represents the GNIP data, and the red line our results from LMDZ-iso.

movement causes the bomb peak in the modeled precipitation to be higher than in the observations. The model then estimates a massive removal of the tritium by the oceans (depending on the water flux exchanges with the ocean surface, whose tritium content is defined as boundary conditions, and on the tritium radioactive decay), faster than deduced from the GNIP data set. The origins of this discrepancy are analyzed in more detail in section 4 with different sensitivity tests.

For the Southern Hemisphere, our simulated tritium outputs exhibit smoother variations during this period, confirmed by the data (Figure 4). For example, the observations from Melbourne show a decrease by a factor of 10 between the maxima in 1965 and 2008, which is very small compared to the stations in the Northern Hemisphere (almost 3 orders of magnitude). This is because most of the nuclear tests were carried out in the Northern Hemisphere. This is expressed by a gentle increase of tritium in precipitation in the Southern Hemisphere until 1962, a rather stable phase from 1963 to 1970, and then a decrease until the end of the simulation in 2008. At the Melbourne station, our simulated tritium in precipitation is in rather good agreement with the data during the maximum phase between 1963 and 1968. However, when the decrease begins at the

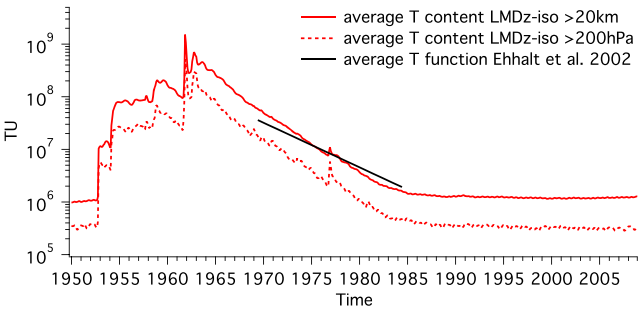

Figure 5. Simulated average tritium in water vapor above 200 hPa level (red dotted line) and 20 km (red solid line) vertical levels during the period 1950–2008 and comparisons with the average tritium function from *Ehhalt et al.* [2002] (black line) based on measurements of tritium in stratospheric water vapor above 20 km altitude.

end of the 1960s, LMDZ-iso again underestimates tritium in precipitation due to the more steeply decreasing slope, which is greater in the simulation than in the data. The consequence is a difference by a factor of 5 between LMDZ-iso and the observations in 2008 in Melbourne. At Halley Bay, on the Antarctic coast, the decrease of the simulated tritium in precipitation from 1968 is again too strong compared to the data. However, there are some differences compared to the situation in Melbourne. Indeed, our simulation overestimates the tritium in precipitation at this station during the maximum phase but agrees quite well with the data from 1990 to 2008. We observe that this period does not present any trend in our simulation nor in the data. These special patterns are certainly due to the unique characteristics of Antarctica from the climatological (cold and dry) and meteorological (polar vortex during the austral winter which isolates the continent from marine air masses) points of view; these characteristics maximize the effects of the stratospheric intrusions of air masses with high tritium content on the local atmospheric tritium concentration.

The seasonal variations observed in the tritium outputs from LMDZ-iso have been analyzed in our previous study [*Cauquoin et al.*, 2015] and are the same after adding the anthropogenic production of tritium. Briefly, in the Northern Hemisphere, there are some discrepancies between data and model outputs with a few months shift in the seasonal maximum of tritium, possibly due to the intensity of baroclinic systems specially in wintertime. In Antarctica, the seasonal maximum takes place during the austral winter in both data and model outputs, but LMDZ-iso overestimates the amplitude of this seasonal cycle. This is possibly because the tritium-rich intruding air in LMDZ-iso spreads out too much in the horizontal [*Hourdin and Armengaud*, 1999], which thus reaches the coastal Antarctic area and the near ocean that should otherwise be less influenced by these stratospheric inputs.

3.2. Tritium in Stratospheric Water Vapor

Because of the importance of stratospheric dynamics in the response of the hydrological cycle to the bomb tritium forcing, we display the picture of the average content of simulated tritium in water vapor above the 200 hPa level and above 20 km high (Figure 5) during the 1950–2008 period. We have chosen these levels because they represent the average pressure level of the tropopause and the minimal height of tritium data from *Ehhalt et al.* [2002], respectively. Above the height of 20 km, the latitudinal variability of our average modeled values of tritium is less than 20%. As described previously, the measurements of tritium in stratospheric water vapor are very limited in time and space, which makes the comparison with our simulation less conclusive. However, it is interesting to observe how fast anthropogenic tritium injected into the upper atmosphere is transported into lower layers to be diluted by the hydrological cycle and the oceans. The pre-bomb level of our simulated tritium in water vapor in the stratosphere is around $2-2.5 \times 10^5$ TU, on the low side of the range of values estimated by *Ehhalt et al.* [2002] and *Fourré et al.* [2006], 5×10^5 TU and 9×10^5 TU, respectively, based on a small number of stratospheric measurements made prior to 1984. The simulated tritium content in stratospheric water vapor increases dramatically from November 1952 to July 1954 by 2 orders of magnitude, in response to the more than 47 kg of tritium injected in the atmosphere during this period of time. This increase is followed by a relatively stable phase until July 1961 and then a sharp increase by a factor of 10 mainly due to the huge amount of tritium (more than 100 kg) released in the atmosphere by the explosion of the Tsar Bomba on 30 October 1961. Tritium in the stratospheric water vapor then continuously decreases from the end of 1962, to finally reach the pre-bomb level and remain stable between 1990 and 2008. The comparison of our simulation with the fit to the stratospheric tritium data from *Ehhalt et al.* [2002] between 1970 and 1985 shows that (1) the average values of tritium in water vapor above the 20 km level from LMDZ-iso agree well with the data, but (2) the simulated decrease of tritium after the bomb peak appears too strong, consistent with our previous conclusions on the tritium in precipitation simulated by LMDZ-iso.

4. Discussion: What Drives the Temporal Evolution of Tritium in Water Vapor and in Precipitation?

In this section, we use the comparison of the patterns of observed and modeled temporal variability of tritium in water since 1950 to examine the driving mechanisms. We report the influences of the height of anthropogenic tritium injection, tritium concentration at the ocean surface, and parameterization of the advection scheme on the global distribution of tritium in water vapor and in precipitation, and especially how they affect the time response of the modeled hydrological cycle with respect to the bomb tritium forcing, i.e., the amplitude of the tritium peak and its decay with time.

4.1. Influences of the Injection Height of Anthropogenic Tritium and of the Prescribed Concentration at the Ocean Surface

One of the main uncertainties concerning the bomb tritium forcing prescribed in our model is not so much the quantity of tritium released into the atmosphere but rather its height of injection in the nuclear cloud. Indeed, tritium injected into the stratosphere is supposed to stay several years in that layer before crossing the tropopause [*Ehhalt et al.*, 2002; *Diallo et al.*, 2012]; in contrast, tritium emitted into the troposphere is rapidly diluted by the hydrological cycle and especially by the oceans. The ocean boundary condition, i.e., the prescribed tritium concentration at the ocean surface, can also have an impact on our modeled concentrations of tritium in water vapor and precipitation through tritium exchanges between the lowest atmospheric layers and the ocean [*Cauquoin et al.*, 2015]. Figure 6 shows the tritium in precipitation from the standard, cloud_top, and 0.2TU simulations between 1950 and 2008, as well as the GNIP data for the different stations reported in section 2.5. For clarity, the data were smoothed to give a 1 year moving average. We also show the modeled tritium in stratospheric water vapor for these different sensitivity tests.

Changing the boundary conditions at the ocean surface has only a small effect on the values of tritium in precipitation, especially before the beginning of the 1980s when the anthropogenic component of tritium in the atmosphere is at its maximum. After this period, which was completely dominated by anthropogenic production, imposing a constant value of 0.2 TU at the surface of the oceans instead of using our reconstructed oceanic boundary conditions results in (1) lower values of tritium in precipitation and (2) the pre-bomb level being reached earlier compared to the standard simulation, especially in the Northern Hemisphere stations, where the difference between the standard and 0.2TU boundary condition is the greatest. This difference is even stronger for the Valentia station, a coastal site in the Northern Hemisphere, because of the greater influence of the ocean on this type of site. In agreement with our previous work [*Cauquoin et al.*, 2015], changing the tritium boundary conditions at the ocean surface has almost no effect on the Antarctic station. As expected, the tritium in stratospheric water vapor from the standard and the 0.2TU simulations are very similar, because this sensitivity test is focused on the surface conditions.

Modifying the height of injection of the anthropogenic tritium in the cloud_top simulation can lead to important changes in the simulated tritium content in precipitation. Indeed, artificially injecting the bomb tritium at higher altitude and in one atmospheric vertical layer only means that tritium will be concentrated in a smaller air volume. Focusing on the Northern Hemisphere stations, we can notice that the first significant increase in tritium in precipitation, which takes place in November 1952 in the standard simulation, is lagged by more than 1 year in the cloud_top simulation. From this increase until the 1990s, except at the time of the bomb peak, the tritium in precipitation from the cloud_top simulation is higher than the one from the standard simulation. The main difference between both simulations for the Northern Hemisphere stations happens during and after the bomb peak with a simulated tritium content higher than the observations until the year 1969 instead of the abrupt decrease suggested in the standard simulation, with a little smaller (e.g., by 16% at Vienna) and broader bomb peak. The situation is rather similar for the Southern Hemisphere with higher tritium contents in precipitation in the cloud_top simulation than in the standard one until the 1990s. From this period, the tritium level in precipitation at all stations in the cloud_top simulation becomes very similar to the tritium values in the standard parameterization. This statement means that the decrease in modeled tritium content in precipitation is still too strong in response to the bomb forcing. However, by concentrating all tritium input in the higher layers of the stratosphere, we would expect smoother variations in modeled tritium of precipitation because of the time needed for downward advection and mixing within the stratosphere.

As expected, one of the main effects of injecting anthropogenic tritium at higher altitude (i.e., more tritium in the stratosphere compared to the standard simulation) is a significant increase of the tritium amount in stratospheric water vapor compared to the standard simulation outputs, by up to a factor of 11

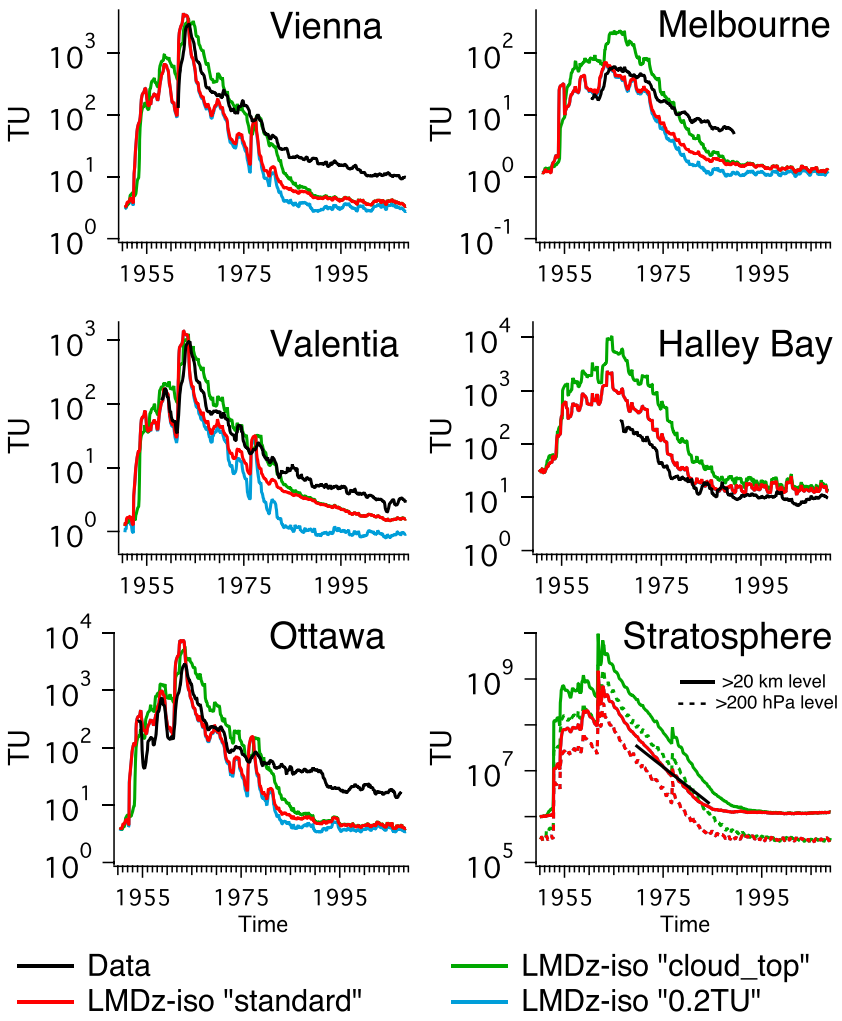

Figure 6. One year moving average tritium in precipitation at the five GNIP stations and average tritium in stratospheric water vapor between 1950 and 2008 in our different simulations (red: standard, green: cloud_top, blue: 0.2TU) and comparison with the available data (black line). For Halley Bay and the stratospheric compartment, the tritium curve from the 0.2TU simulation is merged with the one from the standard simulation.

(average tritium in water vapor above 20 km) during the first important nuclear tests in 1953–1954. We highlight two points about the decrease of tritium level in stratospheric water vapor after the bomb peak. First, the average tritium concentration in water vapor above the 20 km level from the cloud_top simulation is too high compared to the tritium data from *Ehhalt et al.* [2002] (by a factor of ~6). Second, the mean exponential decay time τ of tritium in the stratosphere (for both above the 200 hPa and 20 km levels) between the years 1964 and 1983 is almost the same for the standard and cloud_top simulations: 3.33 and 3.21 years, respectively, which comes to 4.10 and 3.91 years when accounting for the radioactive decay of tritium. If we restrict the analysis to the period between the years 1975 and 1983, we obtain rather similar decay times of 4.82 and 3.91, respectively. Even taking into account some uncertainties related to variations of stratospheric H_2O [*Ehhalt et al.*, 2002] or additional contributions from atmospheric nuclear tests after the bomb peak (until 1980 in our tritium input function), our estimated decay times are clearly smaller than the value of $\tau = 7.7 \pm 2.0$ years from *Ehhalt et al.* [2002]. This indicates that the simulated atmospheric transport of tritium from the stratosphere to the troposphere through the hydrological cycle is too fast, which would explain the too strong decrease of tritium in precipitation after the bomb peak.

4.2. Influence of the Advection Scheme

The previous section highlighted the possible effect of the downward advection between the stratospheric and tropospheric layers on the modeled tritium concentration in precipitation. For instance, the choice of the vertical advection scheme could have a large impact on the residence time of tritium in the stratosphere,

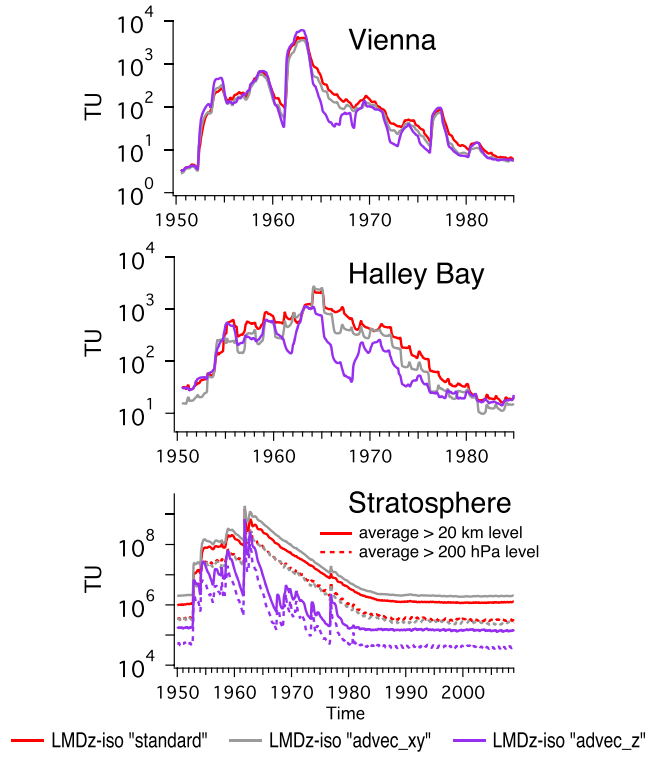

Figure 7. Comparison of the simulated outputs of tritium at Vienna, Halley Bay, and in the stratosphere during the period 1950–2008 between the standard (red), advec_xy (gray) and advec_z (purple) simulations. The curves of precipitation in tritium at Vienna and Halley Bay are smoothed with a 1 year moving average.

as already investigated by *Eluszkiewicz et al.* [2000] for other tracers. So one way to elucidate this effect on our simulated tritium outputs is to modify the advection transport scheme. The resulting changes in the general circulation are very minor since our simulations are nudged by reanalyzed winds. Thus, in Figure 7, we compare the tritium outputs from the simulations advec_xy (upstream horizontal advection) and advec_z (upstream vertical advection) with the ones from our standard simulation. The results from the advec_xy simulation are relatively close to the tritium outputs from the standard one, with a very similar picture of the tritium in stratospheric water vapor. The values of the tritium concentration in precipitation and in high stratospheric water vapor from the advec_xy simulation are slightly lower and higher, respectively, than those from our standard parameterization. In the highest atmospheric vertical layers, a stronger diffusion in the horizontal smooths the latitudinal dependency of tritium (the cosmogenic production term is more important in the higher latitudes) and amplifies the stratification with the consequence of a drier air, which increases slightly the average tritium content in stratospheric water vapor. Closer to the surface, the water vapor at the ocean level diffuses more in the horizontal decreasing the tritium concentration in precipitation and in surface water vapor.

Applying an upstream scheme to the vertical direction (advec_z) leads to a larger difference in our simulated content of tritium in water compared to the standard simulation. Indeed, the variations of tritium concentration in precipitation due to the incorporation of bomb tritium and to its elimination by the hydrological cycle are more abrupt with this assumption, both in time and amplitude. For example, the decay of tritium in precipitation between the bomb peak to year 1968 for Vienna and Halley Bay is stronger than with the standard simulation. Also, the 1 year moving average maximum tritium peak in Vienna has been increased by 50% using this simpler implementation.

The parameterization in the advec_z simulation strongly affects our modeled concentration of tritium in stratospheric water vapor, too. Note that with this simpler implementation the stratospheric water vapor has a lower concentration of tritium. For example, the pre-bomb values are ~7–8 times lower in the advec_z configuration than in the standard one. The temporal shape of tritium in stratospheric water vapor is also greatly impacted, with a more abrupt decrease after each significant injection of bomb tritium into the atmosphere.

For example, the mean decay time of tritium in stratospheric water vapor between 1963 and mid-1967 is equal to only 9 months in the advec_z simulation, clearly lower than the value of 3 years deduced from the standard simulation during the same time period. This behavior also has the consequence that the simulated tritium content of water in the stratosphere is rather stable and reaches the pre-bomb value in 1984, 6 years earlier than in the standard simulation.

These findings confirm that the quality of the simulation of vertical advection is crucial if the model is to reasonably reproduce the temporal evolution of tritium content in the water cycle in response to the nuclear bomb transient forcing. *Meloen et al.* [2003] showed that the AGCMs are influenced by excessive numerical diffusion leading to an artificially too strong downward transport of stratospheric tracers. The modeled transport of tritium with its variations by several orders of amplitude between the stratosphere and the surface makes this tracer very sensitive to this too diffusive vertical advection scheme in LMDZ. So an approach combining tritium data and its modeling provides an additional and valuable test on atmospheric transport models [*Ehhalt et al.*, 2002; *Waugh and Hall*, 2002].

5. Conclusion and Perspectives

We have implemented bomb tritium in the LMDZ-iso model, following our previous work on the implementation of natural tritium in this AGCM [*Cauquoin et al.*, 2015]. This development is the first detailed AGCM modeling of the tritium content of water with the nuclear bomb forcing. It creates a great opportunity to evaluate the model over several decades as the bomb tritium transient signal moves through the hydrological cycle, causing huge variations in the tritium content, i.e., by several orders of magnitude. We have developed a detailed bomb tritium input function (dates, locations, altitudes, and yields). Indeed for the first time, the anthropogenic tritium injected by each of the atmospheric nuclear bomb tests between 1945 and 1980 has been first estimated and further implemented in the model. We have studied the temporal variability of tritium in precipitation and in stratospheric water vapor over a long simulation period with the bomb tritium input function, proper climatic forcing, and tritium boundary conditions at the ocean surface. We have used a comprehensive compilation of published data for tritium in precipitation [*IAEA*, 2016] to evaluate the model performance in terms of amplitude and time response to this anthropogenic forcing. A validation has also been performed for the tritium content in the stratospheric water vapor based on the small number of stratospheric measurements available [*Ehhalt et al.*, 2002].

LMDZ-iso reproduces the general shape of the temporal evolution of tritium between 1950 and 2008 reasonably well, even if some major features need to be improved. However, LMDZ-iso simulates too high a tritium peak at the beginning of the 1960s in the Northern Hemisphere. This modeled peak is also followed by too strong a decrease of tritium in precipitation so that the modeled tritium content in precipitation reaches the pre-bomb level several years sooner than in reality. The average decay time in stratospheric water with the standard simulation, namely, 4.10 years, is significantly lower than the value of 7.7 years from *Ehhalt et al.* [2002].

Our boundary condition on tritium at the ocean surface has little effect during the period 1950–1980 because of the dominant contribution of anthropogenic tritium injected by the high-yield atmospheric thermonuclear tests. We have performed several tests showing that the choice of the vertical advection scheme, with only very minor changes in the general circulation, has the largest effect on the residence time of tritium in the stratosphere, as previously demonstrated by *Eluszkiewicz et al.* [2000] for other tracers. Moreover, the too diffusive vertical advection in the AGCMs [*Meloen et al.*, 2003], and so in LMDZ, has huge consequences on tritium distribution in the troposphere with tritium content in precipitation too high at the bomb peak and too low after 1990. This mismatch with data is even larger when all the tritium is injected into the highest stratospheric layer (cloud_top simulation). Both large-scale features of the circulation and numerical diffusion appear to have a role in influencing mean residence time in the stratosphere [*Hall et al.*, 1999; *Eluszkiewicz et al.*, 2000]; the tritium model-data comparisons provide an additional and valuable test on atmospheric transport models for this issue [*Ehhalt et al.*, 2002; *Waugh and Hall*, 2002].

In conclusion, the incorporation of tritium into an AGCM, from both its natural [*Cauquoin et al.*, 2015] and anthropogenic (this study) origins, creates a new and valuable way of testing the modeled water vapor dynamics, complementing water stable isotope modeling. One of the major advantages of the anthropogenic tritium implementation is the possibility of evaluating the response of the modeled water cycle to a

significant transient forcing over several decades. The AGCMs disperse the stratospheric tracers over too large areas and too deeply into the troposphere, which is likely an artifact from numerical diffusion. In consequence, the AGCMs tend to overestimate the downward transport from the stratosphere to the troposphere [*Meloen et al.*, 2003; *Stohl et al.*, 2003]. This has important consequences on the modeling of tritium in the LMDZ model and more generally on the modeling of the water distribution in the atmosphere. Despite the cost in computing time, one solution could be to increase the vertical resolution, especially in the stratosphere [*Land et al.*, 2002; *Meloen et al.*, 2003; *Stevens et al.*, 2013]. Repeating this work by modeling tritium in another AGCM with another advection scheme, or after having implemented a more advanced (higher-order) scheme in LMDZ, would be useful too [*Eluszkiewicz et al.*, 2000]. Further, a more accurate isotopic modeling of tritium would be useful in revealing the links between the hydrological cycle and the atmospheric dynamics. An approach combining several isotopic proxies (tritium and water stable isotopes) and comparing model simulations with high-resolution data would be particularly valuable. New insight could be expected, for example, from Antarctica, an area with extreme meteorological conditions, where the stratospheric intrusions of air masses have a maximum effect on the local air tritium concentration, especially during the presence of a polar vortex each austral winter.

Appendix A: Comparison of Van Leer's and Upstream Advection Schemes

For simplicity, we consider the advection along one dimension only, with wind flowing from grid box $i-1$ to grid box i and from grid box i to grid box $i+1$. In both *van Leer* [1977] second-order advection scheme and the upstream advection scheme [*Godunov*, 1959], the mixing ratio after advection in box i (q_i') is given by

$$q_i' = \frac{q_i \times m_i + U_{i-1/2} \times q_{i-1/2} - U_{1+1/2} \times q_{i+1/2}}{m_i + U_{i-1/2} - U_{1+1/2}} \tag{A1}$$

where q_i and m_i are the mixing ratio and air mass in box i, $U_{i-1/2}$ is the air mass flux at the boundary between boxes i and $i-1$, and $U_{i+1/2}$ is the air mass flux at the boundary between boxes i and $i+1$. The two schemes differ in the way the water vapor mixing ratio that is advected from box $i-1$ to i, $q_{i-1/2}$, and the water vapor mixing ratio that is advected from box i to $i+1$, $q_{i+1/2}$, are calculated.

In van Leer's scheme, $q_{i-1/2}$ is a linear combination of the mixing ratio in the boxes $i-1$ and i. Similarly, $q_{i+1/2}$ is a linear combination of the mixing ratio in the boxes i and $i+1$. For example, if the air mass flux from grid box $i-1$ to grid box i is very small, then $q_{i-1/2} = (q_i + q_{i-1})/2$. This reflects the air that is advected into box i being restricted to a small margin along the $i-1/i$ boundary, so that its mixing ratio is exactly intermediate between q_{i-1} and q_i.

In contrast, the upstream scheme is much simpler: $q_{i-1/2} = q_{i-1}$ and $q_{i+1/2} = q_i$. This means that even if the air mass flux from grid box $i-1$ to grid box i is very small, the air that is advected into box i has the same water vapor mixing ratio as grid box $i-1$ as a whole. This makes the upstream scheme much more diffusive.

Acknowledgments

We thank three anonymous reviewers for their useful comments that helped to improve this manuscript. The research leading to these results has received funding from the European Research Council under the European Union's Seventh Framework Programme (FP7/2007–2013)/ERC grant agreement no. 306045. LMDZ simulations have been performed on the Ada machine at the IDRIS computing center under the GENCI project 0292. The data sources used in this manuscript are listed in the references and in the supporting information. The table reporting the bomb tritium amount injected into the atmosphere for each atmospheric nuclear bomb test can be downloaded separately in the supporting information and is also available on the PANGAEA database: https://doi.pangaea.de/10.1594/PANGAEA.864909.

References

Andrié, C., P. Jean-Baptiste, and L. Merlivat (1988), Tritium and helium 3 in the northeastern Atlantic Ocean during the 1983 TOPOGULF cruise, *J. Geophys. Res.*, *93*, 12,511–12,524, doi:10.1029/JC093iC10p12511.

Bainbridge, A. E. (1963), Tritium in the North Pacific surface water, *J. Geophys. Res.*, *68*, 3785–3789.

Bonisch, G., and P. Schlosser (1995), Deep water formation and exchange rates in the Greenland/Norwegian Seas and the Eurasian Basin of the Arctic Ocean derived from tracer balances, *Prog. Oceanog.*, *35*, 29–52.

Bony, S., and K. A. Emanuel (2001), A parameterization of the cloudiness associated with cumulus convection; evaluation using TOGA COARE data, *J. Atmos. Sci.*, *58*, 3158–3183, doi:10.1175/1520-0469(2001)058<3158:APOTCA>2.0.CO;2.

Bony, S., C. Risi, and F. Vimeux (2008), Influence of convective processes on the isotopic composition (δ^{18}O and δD) of precipitation and water vapor in the tropics: 1. Radiative-convective equilibrium and Tropical Ocean-Global Atmosphere-Coupled Ocean-Atmosphere Response Experiment (TOGA-COARE) simulations, *J. Geophys. Res.*, *113*, D19305, doi:10.1029/2008JD009942.

Bowen, V. T., and W. Roether (1973), Vertical distributions of strontium 90, cesium 137, and tritium near 45° north in the Atlantic, *J. Geophys. Res.*, *78*, 6277–6285, doi:10.1029/JC078i027p06277.

Broecker, W. S., T. H. Peng, and G. Ostlund (1986), The distribution of bomb tritium in the ocean, *J. Geophys. Res.*, *91*, 14,331–14,344, doi:10.1029/JC091iC12p14331.

Cauquoin, A., P. Jean-Baptiste, C. Risi, É. Fourré, B. Stenni, and A. Landais (2015), The global distribution of natural tritium in precipitation simulated with an Atmospheric General Circulation Model and comparison with observations, *Earth Planet. Sci. Lett.*, *427*, 160–170, doi:10.1016/j.epsl.2015.06.043.

CCHDO (2016), CLIVAR Carbon and Hydrographic Data Office database: WOCE program. [Available at: http://cchdo.ucsd.edu.]

Chadwick, M., et al. (2011), ENDF/B-VII.1 nuclear data for science and technology: Cross sections, covariances, fission product yields and decay data, *Nucl. Data Sheets*, *112*(12), 2887–2996, doi:10.1016/j.nds.2011.11.002.

Compo, G. P., et al. (2011), The Twentieth Century Reanalysis Project, *Q. J. R. Meteorol. Soc.*, *137*, 1–28, doi:10.1002/qj.776.

Constant, P., L. Poissant, and R. Villemur (2009), Tropospheric H(2) budget and the response of its soil uptake under the changing environment, *Sci. Total Environ*, *407*(6), 1809–1823, doi:10.1016/j.scitotenv.2008.10.064.
Craig, H., and D. Lal (1961), The production rate of natural tritium, *Tellus*, *13*(1), 85–105, doi:10.1111/j.2153-3490.1961.tb00068.x.
Diallo, M., B. Legras, and A. Chédin (2012), Age of stratospheric air in the ERA-Interim, *Atmos. Chem. Phys.*, *12*, 12,133–12,154, doi:10.5194/acp-12-12133-2012.
Dockins, K. O., A. E. Bainbridge, J. C. Houtermans, and H. E. Suess (1967), Tritium in the mixed layer of the North Pacific Ocean, in *Radioactive Dating and Methods of Low-Level Counting*, pp. 129–142, IAEA, Vienna.
Dorsey, H. G., and W. H. Peterson (1976), Tritium in the Arctic Ocean and East Greenland Current, *Earth Planet. Sci. Lett.*, *32*, 342–350, doi:10.1016/0012-821X(76)90074-1.
Dreisigacker, E., and W. Roether (1978), Tritium and ^{90}Sr in North Atlantic surface water, *Earth Planet. Sci. Lett.*, *38*(2), 301–312, doi:10.1016/0012-821X(78)90104-8.
Dufresne, J.-L., et al. (2013), Climate change projections using the IPSL-CM5 Earth System Model: From CMIP3 to CMIP5, *Clim. Dynam.*, *40*, 2123–2165, doi:10.1007/s00382-012-1636-1.
Ehhalt, D. H., F. Rohrer, S. Schauffler, and W. Pollock (2002), Tritiated water vapor in the stratosphere: Vertical profiles and residence time, *J. Geophys. Res.*, *107*, 4757, doi:10.1029/2001JD001343.
Eluszkiewicz, J., R. S. Hemler, J. D. Mahlman, L. Bruhwiler, and L. L. Takacs (2000), Sensitivity of age-of-air calculations to the choice of advection scheme, *J. Atmos. Sci.*, *57*, 3185–3201, doi:10.1175/1520-0469(2000)057<3185:SOAOAC>2.0.CO;2.
Emanuel, K. A. (1991), A scheme for representing cumulus convection in large-scale models, *J. Atmos. Sci.*, *48*, 2313–2329, doi:10.1175/1520-0469(1991)048<2313:ASFRCC>2.0.CO;2.
Eriksson, E. (1965), An account of the major pulses of tritium and their effects in the atmosphere, *Tellus*, *17*(1), 118–130, doi:10.1111/j.2153-3490.1965.tb00201.x.
Fourré, E., P. Jean-Baptiste, A. Dapoigny, D. Baumier, J.-R. Petit, and J. Jouzel (2006), Past and recent tritium levels in Arctic and Antarctic polar caps, *Earth Planet. Sci. Lett.*, *245*, 56–64, doi:10.1016/j.epsl.2006.03.003.
Gargett, A. E., G. Östlund, and C. S. Wong (1986), Tritium time series from ocean station P, *J. Physical Oceanogr.*, *16*, 1720–1726, doi:10.1175/1520-0485(1986)016<1720:TTSFOS>2.0.CO;2.
Gat, J. R., W. G. Mook, and H. J. Meijer (2001), Atmospheric water, in *Environmental Isotopes in the Hydrological Cycle—Principles and Applications*, vol. 2, edited by W. G. Mook, 113 pp., UNESCO–IAEA, Paris.
Godunov, S. K. (1959), Finite-difference methods for the numerical computations of equations of gas dynamics, *Math. Sb*, *7*, 271–290.
Hall, T. M., D. W. Waugh, K. A. Boering, and R. A. Plumb (1999), Evaluation of transport in stratospheric models, *J. Geophys. Res.*, *104*, 18,815–18,839, doi:10.1029/1999JD900226.
Happell, J. D., G. Östlund, and A. S. Mason (2004), A history of atmospheric tritium gas (HT) 1950–2002, *Tellus*, *56B*, 183–193, doi:10.1111/j.1600-0889.2004.00103.x.
Hauglustaine, D. A., and D. H. Ehhalt (2002), A three-dimensional model of molecular hydrogen in the troposphere, *J. Geophys. Res.*, *107*, 4330, doi:10.1029/2001JD001156.
Hesshaimer, V., M. Heimann, and I. Levin (1994), Radiocarbon evidence for a smaller oceanic carbon dioxide sink than previously believed, *Nature*, *370*, 201–203, doi:10.1038/370201a0.
Hoffmann, G., M. Werner, and M. Heimann (1998), Water isotope module of the ECHAM atmospheric general circulation model: A study on timescales from days to several years, *J. Geophys. Res.*, *103*(D14), 16,871–16,896, doi:10.1029/98JD00423.
Hourdin, F., and A. Armengaud (1999), The use of finite-volume methods for atmospheric advection of trace species. Part I: Test of various formulations in a general circulation model, *Mon. Weather Rev.*, *127*(5), 822–837, doi:10.1175/1520-0493(1999)127<0822:TUOFVM>2.0.CO;2.
Hourdin, F., et al. (2006), The LMDZ4 general circulation model: Climate performance and sensitivity to parametrized physics with emphasis on tropical convection, *Clim. Dynam.*, *27*, 787–813, doi:10.1007/s00382-006-0158-0.
Hourdin, F., et al. (2013), Impact of the LMDZ atmospheric grid configuration on the climate and sensitivity of the IPSL-CM5A coupled model, *Clim. Dynam.*, *40*, 2167–2192, doi:10.1007/s00382-012-1411-3.
IAEA (2016), International Atomic Energy Agency/World Meteorological Organization. Global Network of Isotopes in Precipitation (GNIP) Database. [Available at: https://nucleus.iaea.org/wiser.]
Jain, A. K., H. S. Kheshgi, and D. J. Wuebbles (1997), Is there an imbalance in the global budget of bomb-produced radiocarbon?, *J. Geophys. Res.*, *102*, 1327–1333, doi:10.1029/96JD03092.
Jean-Baptiste, P., A. Dapoigny, and J. J. Poupeau (1998), North-eastern Atlantic ^{3}He and tritium data: The BORD-EST expedition 1988. Data Release n°6, Tech. Rep., LSCE, CEA-Saclay, F-91191 - Gif/Yvette.
Jean-Baptiste, P., W. J. Jenkins, J. C. Dutay, E. Fourré, V. Leboucher, and M. Fieux (2004), Temporally integrated estimate of the Indonesian throughflow using tritium, *Geophys. Res. Lett.*, *31*, L21301, doi:10.1029/2004GL020854.
Jean-Baptiste, P., D. Baumier, E. Fourré, A. Dapoigny, and B. Clavel (2007), The distribution of tritium in the terrestrial and aquatic environments of the Creys-Malville nuclear power plant (2002–2005), *J. Environ. Radioact.*, *94*(2), 107–118, doi:10.1016/j.jenvrad.2007.01.010.
Jenkins, W. J. (1977), Tritium-helium dating in the Sargasso Sea: A measurement of oxygen utilization rates, *Science*, *196*, 291–292, doi:10.1126/science.196.4287.291.
Jenkins, W. J. (1980), Tritium and ^{3}He in the Sargasso Sea, *J. Mar. Res.*, *38*, 533–569.
Jenkins, W. J. (1989), Helium Isotope Laboratory Data Release 3.0: 1981 Results TTO, Tech. Rep., Woods Hole Oceanographic Institution.
Jenkins, W. J. (1996), Tritium and ^{3}He in the WOCE Pacific Program, *Int. WOCE Newslett.*, *23*, 6–8.
Joussaume, S., R. Sadourny, and J. Jouzel (1984), A general circulation model of water isotope cycles in the atmosphere, *Nature*, *311*, 24–29, doi:10.1038/311024a0.
Jouzel, J., and L. Merlivat (1984), Deuterium and oxygen 18 in precipitation: Modeling of the isotopic effects during snow formation, *J. Geophys. Res.*, *89*, 11,749–11,757, doi:10.1029/JD089iD07p11749.
Jouzel, J., L. Merlivat, M. Pourchet, and C. Lorius (1979), A continuous record of artificial tritium fallout at the South Pole (1954–1978), *Earth Planet. Sci. Lett.*, *45*, 188–200, doi:10.1016/0012-821X(79)90120-1.
Jouzel, J., L. Merlivat, D. Mazaudier, M. Pourchet, and C. Lorius (1982), Natural tritium deposition over Antarctica and estimation of the mean global production rate, *Geophys. Res. Lett.*, *9*, 1191–1194, doi:10.1029/GL009i010p01191.
Jouzel, J., G. L. Russell, R. J. Suozzo, R. D. Koster, J. W. C. White, and W. S. Broecker (1987), Simulations of the HDO and $H_2^{18}O$ atmospheric cycles using the NASA/GISS general circulation model: The seasonal cycle for present-day conditions, *J. Geophys. Res.*, *92*, 14,739–14,760, doi:10.1029/JD092iD12p14739.

Kakiuchi, H., N. Momoshima, T. Okai, and Y. Maeda (1999), Tritium concentration in ocean, *J. Radioanal. Nucl. Chem.*, *239*(3), 523–526, doi:10.1007/BF02349062.
Kellogg, W. W., R. R. Rapp, and S. M. Greenfield (1957), Close-in fallout., *J. Atmos. Sci.*, *14*, 1–8, doi:10.1175/0095-9634-14.1.1.
Koster, R. D., W. S. Broecker, J. Jouzel, R. J. Suozzo, G. L. Russell, D. Rind, and J. W. C. White (1989), The global geochemistry of bomb-produced tritium: General circulation model compared to available observations and traditional interpretations, *J. Geophys. Res.*, *94*, 18,305–18,326, doi:10.1029/JD094iD15p18305.
Land, C., J. Feichter, and R. Sausen (2002), Impact of vertical resolution on the transport of passive tracers in the ECHAM4 model, *Tellus*, *54*, 344–360, doi:10.1034/j.1600-0889.2002.201367.x.
Landa, E. R., D. M. Beals, J. E. Halverson, R. L. Michel, and G. R. Cefus (1999), Tritium and plutonium in waters from the Bering and Chukchi Seas, *Health Phys.*, *77*(6), 668–676.
Lassey, K. R., I. G. Enting, and C. M. Trudinger (1996), The Earth's radiocarbon budget. A consistent model of the global carbon and radiocarbon cycles, *Tellus*, *48*, 487–501, doi:10.1034/j.1600-0889.1996.t01-2-00007.x.
Leboucher, V., P. Jean-Baptiste, É. Fourré, M. Arnold, and M. Fieux (2007), Oceanic radiocarbon and tritium on a transect between Australia and Bali (Eastern Indian ocean), *Radiocarbon*, *46*(2), 567–581.
Lee, J.-E., I. Fung, D. J. Depaolo, and C. C. Henning (2007), Analysis of the global distribution of water isotopes using the NCAR atmospheric general circulation model, *J. Geophys. Res.*, *112*, D16306, doi:10.1029/2006JD007657.
Lott, F., L. Fairhead, F. Hourdin, and P. Levan (2005), The stratospheric version of LMDz: Dynamical climatologies, Arctic oscillation, and impact on the surface climate, *Clim. Dynam.*, *25*(7-8), 851–868, doi:10.1007/s00382-005-0064-x.
Lucas, L. L., and M. P. Unterweger (2000), Comprehensive review and critical evaluation of the half-life of tritium, *J. Res. Natl. Inst. Stand. Technol.*, *105*(4), 541–549, doi:10.6028/jres.105.043.
Machta, L. (1950), Entrainment and the maximum height of an atomic cloud, *Bull. Am. Meteorol. Soc.*, *37*, 87–93.
Martell, E. A. (1963), On the inventory of artificial tritium and its occurrence in atmospheric methane, *J. Geophys. Res.*, *68*, 3759–3769.
Masarik, J., and J. Beer (2009), An updated simulation of particle fluxes and cosmogenic nuclide production in the Earth's atmosphere, *J. Geophys. Res.*, *114*, D11103, doi:10.1029/2008JD010557.
Mathieu, R., D. Pollard, J. E. Cole, J. W. C. White, R. S. Webb, and S. L. Thompson (2002), Simulation of stable water isotope variations by the genesis GCM for modern conditions, *J. Geophys. Res.*, *107*(D4), 4037, doi:10.1029/2001JD900255.
Meloen, J., et al. (2003), Stratosphere-troposphere exchange: A model and method intercomparison, *J. Geophys. Res.*, *108*, 8526, doi:10.1029/2002JD002274.
Merlivat, L., and J. Jouzel (1979), Global climatic interpretation of the deuterium-oxygen 18 relationship for precipitation, *J. Geophys. Res.*, *84*(C8), 5029–5033, doi:10.1029/JC084iC08p05029.
Michel, R., and P. M. Williams (1973), Bomb-produced tritium in the Antarctic Ocean, *Earth Planet. Sci. Lett.*, *20*, 381–384, doi:10.1016/0012-821X(73)90013-7.
Michel, R. L. (1976), Tritium inventories of the world oceans and their implications, *Nature*, *263*, 103–106, doi:10.1038/263103a0.
Michel, R. L., and H. E. Suess (1975), Bomb tritium in the Pacific Ocean, *J. Geophys. Res.*, *80*, 4139–4152, doi:10.1029/JC080i030p04139.
Michel, R. L., T. W. Linick, and P. M. Williams (1979), Tritium and carbon-14 distributions in seawater from under the Ross Ice Shelf Project ice hole, *Science*, *203*, 445–446, doi:10.1126/science.203.4379.445.
Miskel, J. A. (1973), Production of tritium by nuclear weapons, in *Tritium*, edited by A. A. Moghissi and M. W. Carter, pp. 79–85, Messenger Graphics Publ., Phoenix, Arizona.
Mulsow, S., P. P. Povinec, B. L. K. Somayajulu, B. Oregioni, L. L. W. Kwong, J. Gastaud, Z. Top, and U. Morgenstern (2003), Temporal (^{3}H) and spatial variations of ^{90}Sr, ^{239,240}Pu and ^{241}Am in the Arabian Sea: GEOSECS Stations revisited, *Deep-Sea Res. II*, *50*, 2761–2775, doi:10.1016/S0967-0645(03)00146-2.
Naegler, T. (2005), The global bomb radiocarbon budget: Simulation and application, PhD thesis, Univ. of Heidelberg.
Naegler, T., and I. Levin (2006), Closing the global radiocarbon budget 1945–2005, *J. Geophys. Res.*, *111*(D10), D12311, doi:10.1029/2005JD006758.
Noone, D., and I. Simmonds (2002), Associations between δ^{18}O of water and climate parameters in a simulation of atmospheric circulation for 1979–95, *J. Clim*, *15*, 3150–3169, doi:10.1175/1520-0442(2002)015<3150:ABOOWA>2.0.CO;2.
NRCP (1979), Tritium in the environment. NRCP No. 62, Tech. Rep., National Council on Radiation Protection and Measurements.
Östlund, H. G., and C. Grall (1987), Transient tracers in the ocean: North and tropical Atlantic tritium and radiocarbon. Tritium Laboratory Data Report no°16, Tech. Rep., Univ. of Miami.
Östlund, H. G., M. O. Rinkel, and C. Rooth (1969), Tritium in the equatorial Atlantic current system, *J. Geophys. Res.*, *74*, 4535–4543, doi:10.1029/JC074i018p04535.
Östlund, H. G., C. Grall, and R. E. Brescher (1986), Equatorial Pacific tritium. Tritium Laboratory Data Report n°15, Tech. Rep., Univ. of Miami.
Östlund, H. G., H. Craig, W. B. Broecker, and D. Spencer (1987), *GEOSECS Atlantic, Pacific, and Indian Ocean Expeditions: Volume 7, Shorebased Data and Graphics*, National Science Foundation, Washington, D. C.
Povinec, P. P., K. Hirose, T. Honda, T. Ito, E. M. Scott, and O. Togawa (2004), Spatial distribution of ^{3}H, ^{90}Sr, ^{137}Cs and ^{239,240}Pu in surface waters of the Pacific and Indian Oceans—GLOMARD database, *J. Environm. Radioact.*, *76*(1–2), 113–137, doi:10.1016/j.jenvrad.2004.03.022.
Risi, C., S. Bony, F. Vimeux, and J. Jouzel (2010), Water-stable isotopes in the LMDZ4 general circulation model: Model evaluation for present-day and past climates and applications to climatic interpretations of tropical isotopic records, *J. Geophys. Res.*, *115*(D14), D12118, doi:10.1029/2009JD013255.
Risi, C., et al. (2012), Process-evaluation of tropospheric humidity simulated by general circulation models using water vapor isotopic observations: 2. Using isotopic diagnostics to understand the mid and upper tropospheric moist bias in the tropics and subtropics, *J. Geophys. Res.*, *117*, D05304, doi:10.1029/2011JD016623.
Risi, C., A. Landais, R. Winkler, and F. Vimeux (2013), Can we determine what controls the spatio-temporal distribution of d-excess and ^{17}O-excess in precipitation using the LMDZ general circulation model?, *Clim. Past*, *9*, 2173–2193, doi:10.5194/cp-9-2173-2013.
Roether, W. (1974), The tritium and carbon-14 profiles at the Geosecs I (1969) and GOGO I (1971) North Pacific stations, *Earth Planet. Sci. Lett.*, *23*, 108–115, doi:10.1016/0012-821X(74)90037-5.
Roether, W., K.-O. Münnich, and H. G. Östlund (1970), Tritium profile at the North Pacific (1969) Geosecs Intercalibration Station, *J. Geophys. Res.*, *75*, 7672–7675, doi:10.1029/JC075i036p07672.
Schell, W. R., S. Sauzay, and B. R. Payne (1974), World distribution of environmental tritium, in *Physical Behaviour of Radioactive Contaminants in the Atmosphere*, pp. 374–385, IAEA, Vienna.
Schlosser, P. (1985), Ozeanographische Anwendungen von spurenstoffmessungen im Mittelmeerausstrom und Europaischen Nordmeer, PhD thesis, Ruprecht-Karls Univ., Heidelberg.

Schlosser, P., G. Bönisch, B. Kromer, H. H. Loosli, B. Bühler, R. Bayer, G. Bonani, and K. P. Kolterman (1995), Mid-1980s distribution of tritium, ^{3}He, ^{14}C and ^{39}Ar in the Greenland/Norwegian Seas and the Nansen Basin of the Arctic Ocean, *Prog. Oceanog.*, *35*(1), 1–28, doi:10.1016/0079-6611(95)00003-Y.

Schmidt, G. A., A. N. Legrande, and G. Hoffmann (2007), Water isotope expressions of intrinsic and forced variability in a coupled ocean-atmosphere model, *J. Geophys. Res.*, *112*, D10103, doi:10.1029/2006JD007781.

Sloth, E. N., D. L. Horrocks, E. J. Hoyce, and M. H. Studier (1962), Tritium in the thermal neutron fission of uranium–235, *J. Inorg. Nucl. Chem.*, *24*(4), 337–341, doi:10.1016/0022-1902(62)80027-X.

Stevens, B., et al. (2013), Atmospheric component of the MPI-M Earth System Model: ECHAM6, *J. Adv. Model. Earth Syst.*, *5*, 146–172, doi:10.1002/jame.20015.

Stohl, A., et al. (2003), Stratosphere-troposphere exchange: A review, and what we have learned from STACCATO, *J. Geophys. Res.*, *108*, 8516, doi:10.1029/2002JD002490.

Tamuly, A. (1974), Dispersal of tritium in Southern Ocean waters, *Arctic*, *27*(1), 27–40, doi:10.14430/arctic2850.

Taylor, C. B. (1968), A comparison of tritium and strontium-90 fallout in the Southern Hemisphere, *Tellus*, *20*, 559–576, doi:10.1111/j.2153-3490.1968.tb00400.x.

Tindall, J. C., P. J. Valdes, and L. C. Sime (2009), Stable water isotopes in HadCM3: Isotopic signature of El Niño-Southern Oscillation and the tropical amount effect, *J. Geophys. Res.*, *114*, D04111, doi:10.1029/2008JD010825.

Top, Z., R. M. Moore, and W. B. Clarke (1998), Variability in deep exchange between the Eurasian and Greenland Basins: Evidence from tritium and helium-3, *Geophys. Res. Lett.*, *25*(9), 1403–1406, doi:10.1029/98GL00951.

United Nations Scientific Committee on the Effects of Atomic Radiation (UNSCEAR) (2000), Reports to the General Assembly, *Tech. Rep.*, United Nation Scientific Committee on the Effects of Atomic Radiations, United Nations, New York.

U.S. Department of Energy Nevada Operations Office (2000), United States Nuclear Tests—July 1945 through September 1992, *Tech. Rep.* DOE/NV–209-Rev 15.

van Leer, B. (1977), Towards the ultimate conservative difference scheme. IV. A new approach to numerical convection, *J. Comput. Phys.*, *23*, 276–299, doi:10.1016/0021-9991(77)90095-X.

Wagenbach, D., M. Legrand, H. Fischer, F. Pichlmayer, and E. W. Wolff (1998), Atmospheric near-surface nitrate at coastal Antarctic sites, *J. Geophys. Res.*, *103*, 11,007–11,020, doi:10.1029/97JD03364.

Warner, F., and R. J. C. Kirchmann (2000), *Nuclear Test Explosions: Environmental and Human Impacts*, vol. SCOPE 59, John Wiley, West Sussex, England.

Waugh, D., and T. Hall (2002), Age of stratospheric air: Theory, observations, and models, *Rev. Geophys.*, *40*(4), 1010, doi:10.1029/2000RG000101.

Weiss, W., and W. Roether (1980), The rates of tritium input to the world oceans, *Earth Planet. Sci. Lett.*, *49*, 435–446, doi:10.1016/0012-821X(80)90084-9.

Werner, M., P. M. Langebroek, T. Carlsen, M. Herold, and G. Lohmann (2011), Stable water isotopes in the ECHAM5 general circulation model: Toward high-resolution isotope modeling on a global scale, *J. Geophys. Res.*, *116*(D15), D15109, doi:10.1029/2011JD015681.

Yoshimura, K., M. Kanamitsu, D. Noone, and T. Oki (2008), Historical isotope simulation using Reanalysis atmospheric data, *J. Geophys. Res.*, *113*, D19108, doi:10.1029/2008JD010074.

Zaucker, F. (1988), ^{3}H/^{3}He Datierung der flachen Wassersaule in Arktischen Ozean, PhD thesis, Inst. fur Umweltphysik, Heidelberg.